Modeling Reactive Geochemical Transport of Concentrated Aqueous Solutions in Variably Saturated Media

Guoxiang Zhang, Zuoping Zheng, Jiamin Wan
Earth Science Division, Lawrence Berkeley National Laboratory, Berkeley, CA 94720

Abstract

Concentrated aqueous solutions (CAS) have unique thermodynamic and physical properties. Chemical components in CAS are incompletely dissociated, especially those containing divalent or polyvalent ions. The problem is further complicated by the interaction between CAS flow processes and the naturally heterogeneous sediments. As the CAS migrates through the porous media, the composition may be altered subject to fluid-rock interactions. To effectively model reactive transport of CAS, we must take into account ion-interaction. A combination of the Pitzer ion-interaction and the ion-association model would be an appropriate way to deal with multiple-component systems if the Pitzer' parameters and thermodynamic data of dissolved components and the related minerals are available. To quantify the complicated coupling of CAS flow and transport, as well as the involved chemical reactions in natural and engineered systems, we have substantially extended an existing reactive biogeochemical transport code, BIO-CORE$^{2D©}$, by incorporating a comprehensive Pitzer ion-interaction model. In the present paper, the model, and two test cases against measured data were briefly introduced. Finally we present an application to simulate a laboratory column experiment studying the leakage of the high alkaline waste fluid stored in Hanford (a site of the U.S. Department of Energy, located in Washington State, USA). With the Pitzer ion-interaction ionic activity model, our simulation captures measured pH evolution. The simulation indicates that all the reactions controlling the pH evolution, including cation exchanges, mineral precipitation and dissolution, are coupled.

Key words: Pitzer, ion-interaction, concentrated aqueous solution, modeling, BIO-CORE$^{2D©}$, Handford, high alkaline waste fluid

1. Introduction

Concentrated aqueous solutions (CAS) are generally referred to aqueous solutions with ionic strength larger than 1 M. CAS occur in many natural and contaminated environments, including seawater evaporation and intrusion (Harvie and Weare, 1980; Harvie et al., 1984; Krumgalz, 2001), industrial kraft pulp mills and bayer processes (Gerson and Zhang, 1997; Park and Englezos, 1999), toxic waste solutions (Van Gaans and Schuiling, 1997; Gephart and Lundgren, 1998), leakage of electrolytic fluids from storage tanks, and acid mine drainage (Blowes et al., 1991). CAS behaves significantly different from dilute solutions in transport and geochemical processes because of their large density, viscosity and complicated ion-interactions. Thus, challenges remain for numerical modeling of CAS, because most geochemical reactive transport models are based on ideal (dilute) aqueous solutions and not applicable to CAS (Pitzer, 1991; Oldenburg and Pruess, 1995). For instance, a significant amount of high-concentration (up to more than 10 M) radioactive waste fluids is leaking from some of the 149 single-shell and 28 double-shell underground tanks at Hanford site. Groundwater system has been contaminated. Study on the migration of the fluids and the contamination on the groundwater system, numerical models dealing with the CAS are key tools.

Pitzer's ion-interaction theory (Pitzer, 1973) has often been used to study ionic activity in CAS. Harvie and Weare (1980) developed an ion-interaction equilibrium model (HWM) for the sea water system (Na-K-Mg-Ca-Cl-SO_4-H_2O) based on the Pitzer's ion-interaction theoretical model. The HWM model was implemented in several computer codes: PHRQPITZ (Plummer et al., 1988), EQ3/6 (Wolery and Daveler, 1992), GMIN (Flemy, 1995), and UNSATCHEM-2D (Simunek and Suarez, 1994). PHRQPITZ extends to include the components Fe(II), Mn, Ba, Sr, Li, and Br under higher temperature (60^{o}C) and pressure, allowing calculations for hydrothermal systems. GMIN and UNSATCHEM-2D also provide an extension to the HWM by including borate components. Recently, based on previous studies, Risacher and Clement (2001) presented a pure chemical equilibrium model (EQL/EVP) for simulating evaporation of natural waters at high concentration. To estimate tank supernate compositions from historical tank inventory data at the Hanford nuclear waste site, Lichtner and Flemy (2002) performed simulations based on a combination of the computer code GMIN (Felmy, 1995) and the reactive transport code FLOTRAN (Lichtner, 2001). Steefel et al. (2003) simulated the multiple cation exchanges taking place in the sediments of

Hanford under highly alkaline conditions. Their simulation confirmed that multisite cation exchange is a very important process in controlling cesium migration in Hanford sediment. Actually, the dynamic behavior of CAS in subsurface environments does not appear as simple thermodynamic equilibrium processes. In a non-equilibrium context, the study of CAS under flowing conditions poses a compelling and challenging problem caused by the higher nonlinearity of the reaction rate. In addition, CAS exerts strong influences on fluid physical properties of the flow such as density and viscosity. A formulation for density- and viscosity-dependent flows in two-dimensional variably saturated media is presented by Monnin (1994) and Boufadel et al. (1998). Several numerical models have been used to simulate transport of CAS (Voss and Souza, 1987; Herbert et al., 1988; Oldenburg and Pruess, 1995). However, most of these models consider only a simple chemistry and neglect ion-interactions. It has been known for decades that thermodynamic properties of CAS (including activity coefficients, osmotic coefficients, and water activity) are significantly different from dilute solutes (Pitzer, 1991). Whether thermodynamic properties of CAS change or not, and how they affect transport processes are not well understood.

The present work was motivated by a modeling study regarding leakage of highly alkaline-saline waste-tank solutions at the U.S. Department of Energy's Hanford site. In this paper, we present (1) mathematical equations of the Pitzer ion-interaction model for calculating activity, (2) the model implementation to the existing biogeochemical computer code, BIO-CORE$^{2D©}$, and (3) the development of a database for the temperature-dependent Pitzer ion-interaction parameters. We then present two test cases, by comparing our numerical results with the reported experimental data of activity coefficients. Finally, we apply of our Pitzer ion-interaction model to a laboratory experiment extracted from the Hanford site in which pH measurements were available for comparison. The application involves unsaturated flow, cation exchanges, and mineral dissolution/precipitation.

2. Pitzer's Ionic Activity Model

In a given chemical solution, the thermodynamic activity of an aqueous species is calculated as the product of the concentration and the activity coefficient. The coefficient of each species is the function of concentrations and ionic radius of all species in the solution. It is also dependent on temperature, not only through the temperature dependency of the chemical species' thermodynamic

properties in the solution, but also the temperature-dependent constants used in the activity coefficient equations.

For nonconcentrated solutions (ionic strength smaller than 1 M), values of the activity coefficient are commonly calculated according to the extended Debye-Hückel formula, which are presented in Appendix A. The excess solution free energy subjected to the interactions between any specific ionic pairs is not considered in the Debye-Hückel formula, and this excess solution free energy becomes significant in high concentration solutions. Therefore, Debye-Hückel formula, expressed as a universal function of the ionic strength rather than any specific ionic species, is not suitable for calculations of ionic activity in CAS (Bethke, 1996).

Ion-interactions in CAS have a major influence on activities of components. A quantitative description of these effects requires a self-consistent model capable of handling the variation of ionic activity coefficients as a function of ionic strength, composition, temperature, and pressure. The Pitzer ion-interaction model (Pitzer, 1973) can accurately quantify the activity coefficients as well as other thermodynamic properties of the CAS as a function of variables mentioned above. These semi-empirical equations are sometimes called virial equations, specific interaction equations, and phenomenological equations. The equations can adequately express the thermodynamic properties over a wide range of concentration and temperature (Clegg and Whitfield, 1991). The Pitzer ion-interaction model, based on a virial expansion (Pitzer, 1973, 1991) is reduced to a modified form of the Debye-Hückel formula at low ionic strength (Pitzer, 1991). This virial expansion involves a sum over all possible binary and ternary short-range interaction terms as well as mixing terms. The accepted form of the Pitzer model has been formulated by Harvie et al. (1984). In these formulations, the pressure dependence is not taken into account. Water activity, a_{H_2o}, osmotic coefficient, ϕ, activity coefficients of the cations, γ_M, anions, γ_X, and neutral species, γ_N are mathematically expressed in the following equations:

$$Ln\, a_{H_2o} = -\frac{W}{1000}\left(\sum_{i=1}^{N_T} m_i\right)\phi \tag{1}$$

$$\sum_{i=1}^{N_T} m_i(\phi - 1) = 2\left(-\frac{A^{\Phi} I^{\frac{3}{2}}}{1 + 1.2\sqrt{I}}\right) + \sum_{c=1}^{N_c}\sum_{a=1}^{N_a} m_c m_a\left(B_{ca}^{\Phi} + ZC_{ca}\right) + \sum_{n=1}^{N_n}\sum_{c=1}^{N_c} m_n m_c \lambda_{nc} + \sum_{n=1}^{N_n}\sum_{a=1}^{N_a} m_n m_a \lambda_{na} \tag{2}$$

$$ln\gamma_M = Z_M^2 F + \sum_{a=1}^{N_a} m_a(2B_{Ma} + ZC_{Ma}) + |Z_M| \sum_{c=1}^{N_c}\sum_{a=1}^{N_a} m_c m_a C_{ca} + 2\sum_{n=1}^{N_n} m_n \lambda_{nM} \quad (3)$$

$$ln\gamma_X = Z_X^2 F + \sum_{c=1}^{N_c} m_c(2B_{cX} + ZC_{cX}) + |Z_x| \sum_{c=1}^{N_c}\sum_{a=1}^{N_a} m_c m_a C_{ca} + 2\sum_{n=1}^{N_n} m_n \lambda_{nX} \quad (4)$$

$$ln\gamma_N = \sum_{a=1}^{N_a} m_a(2\lambda_{Na}) + \sum_{c=1}^{N_c} m_c(2\lambda_{Nc}) \quad (5)$$

where m_i, m_c, and m_a, are the molality of species *i*, *c*, and *a*, respectively; *W* is the molecular weight of water, N_T is the number of species in the system; *I* is the ionic strength; the subscripts *M* and *c* denote cations, *X* and *a* denote anions; *N* and *n* denote neutral species; and *i* denotes all species in the solution. As implied in the equations, the capital *M* and *X* are used to denote the subject ions (e. g. the ion for which the activity coefficient is calculated) while *c* and *a* indicate the cations and anions interacting with the subject ions or with each others. N_c, N_a, and N_n are the numbers of cations, anions and neutral species, respectively, interacting with the subject ions, and normally are the total numbers of the cations, anions and neutral species in the system. Z_M and Z_X are the electrical charges of the subject cation *M* and subject anion *X*, respectively, whereas λ_{na}, λ_{Na} and λ_{nX} are coefficients of the interactions between neutral species and anions, and λ_{nc}, λ_{Nc} and λ_{nM} are the coefficients of the interactions between neutral species and cations.

F is the modified Debye-Hückel term, *Z* is the solution electrical charge, A^{Φ} is one third of the Debye-Hückel limiting slope. B_{ca}^{Φ}, B_{MX} (representing B_{Ma} and B_{cX}), B'_{MX} (representing B'_{Ma} and B'_{cX}), α_{MX}, and C_{MX} (representing C_{Ma}, C_{cX} and C_{ca}) are Pitzer virial coefficients. All of these variables are given in Appendix B.

The mean ionic activity coefficient, $\gamma_{\pm}$, is commonly used for calculating species activity coefficients in CAS and is defined as:

$$Ln\gamma_{\pm} = (\nu_M ln\gamma_M + \nu_X ln\gamma_X)/\nu \quad (6)$$

where ν_M and ν_X are the stoicheomitric coefficients of cations and anions in the compound formula, respectively, and $\nu = \nu_M + \nu_X$.

Note that the binary interactions between ions of like signs, ternary ion of one sign, and two dissimilar ions of opposite signs (regarded as mixing terms) are not considered in the present model, because the mixing terms make relatively much smaller contributions to the activity coefficients than the contributions from the interactions of binary ionic pairs with opposite sings (Pitzer and Kim, 1974). By neglecting the mixing term, computational time is significantly saved — a vital advantage for reactive transport models. As shown in the model test, this simplification does not affect the simulated results significantly.

The volume of a CAS is contributed by water volume, partial volume of solutes, and the excess volume evoked by the ionic interaction. For solutions with ionic strength larger than 0.1 M, the partial volume of solutes and the excess volume become significant. The apparent water density in CAS varies depending on the concentrations (Dougherty, 2001) owing to the ion-water molecule interaction. However, this variation has not been well formulated for complicated solutions and is considered to be a minor contribution to the solution density (Monnin, 1994) comparing with the contribution from solute partial volume and the excess volume. The partial volume of solutes is a linear function of concentration and can be calculated. Note that this calculation must obey the ionic volume conservation law. The excess volume is relevant to the solution free energy change and can also be formulated as a function of concentrations using the Pitzer virial equations (Pitzer, 1991; Monnin, 1994). Accounting for these three contributions, the density of CAS in the present model is calculated using the formulation and the virial parameters given by Monnin (1994). Nine major ions (Na^+, K^+, Ca^{+2}, Mg^{+2}, Cl^-, SO_4^{-2}, HCO_3^-, NO_3^- and CO_3^{-2}) have been considered to significantly contribute to the solution density. Other ions are easy to add into the model if their virial coefficients are known or they can be calibrated by inverting the model.

3. Numerical Implementation

The pitzer ion-interaction model presented above for calculating activity coefficients has been implemented in the existing reactive biogeochemical transport computer code, BIO-CORE$^{2D©}$ (Zhang, 2001) The Debye-Hückel formula is also included in the code. Thus, activity coefficients can be calculated using either the Pitzer model or the Debye-Hückel model according to user option, or an automatic shift between either methods, depending on a prescribed threshold of ionic strength.

The Pitzer model is used for ionic strength greater than 1 M, while the Debye-Hückel modle is used for saving computation time when dealing with low concentrations. BIO-CORE$^{2D©}$ solves the nonlinear algebraic equation system (NAEs) of the chemical system using Newtown-Raphson iteration method, which requires calculating the derivatives of the ionic activity with respect to the concentrations of primary species. These derivatives are analytically derived from Equations (1) through (5) and implemented into the program.

BIO-CORE$^{2D©}$ describes the hydrogeochemical system as the integration of migration and transformation of substance and energy in the subsurface. The simulator can accommodate any number of chemical species, including aqueous and adsorbed species and minerals, and any number of microbiological species, including attached phase and dissolved species (in water). A wide range of subsurface thermo-physical-chemical processes is considered. The major processes considered for fluid and heat flow are: (1) fluid flow in variable saturated media under pressure and gravity forces, (2) capillary pressure effects for the liquid phase, and (3) heat flow by conduction and convection. Transport processes of chemical species considered are advection, molecular diffusion, and hydrodynamic dispersion. A wide range of geochemical reactions is considered, including aqueous complexations, acid-base, redox, mineral dissolution/precipitation, ionic exchanges, and sorptions. Microbial metabolisms and the coupling between the geochemical system and the microbial ecosystem are also considered. Reactions among aqueous chemical species and mass transfer between different phases can be treated under either local equilibrium or kinetic conditions.

A two-dimensional Galerjin finite-element method was used for spatial discretization. The program uses a sequential iteration approach (SIA; *Yeh and Tripathi*, 1991] for solving the coupled system of fluid and heat flow, solute transport, and biogeochemical reactions. The SIA uses the following sequence: water flow, heat transfer, solute transport, equilibrium chemical reactions, kinetic chemical reactions and microbial metabolisms. Solute transport is solved on a chemical component basis. The system of biogeochemical reaction equations is solved on a node-by-node basis by the Newton-Raphson iteration method. The sequences are iteratively solved until convergence. Full details on numerical methods are given in Zhang (2001), Samper et al. (2000), and Xu et al. (1999).

4. Database for the Pitzer Ion-Interaction Parameters

A database for Pitzer ion-interaction model parameters is attached to the program, in addition to the existing thermodynamic and kinetic databases. The parameters of the Pitzer model are usually obtained from laboratory experiments through electromotive force (EMF) and isopetic measurements for binary or ternary electrolytes (Pitzer, 1991). Pitzer and Mayorga (1973) and Pitzer (1991) summarized a number of parameter values at 25^{o}C for major ions. An extensive literature review of the Pitzer ion-interaction parameters for many inorganic salts has been given by Plummer et al. (1988) in a documentation of the computer code PHRQPITZ. The values of Pitzer' parameters in the database of BIO-CORE $^{2D©}$ remain mostly the same as those used in PHRQPITZ. For some ions, virial parameters were taken from other literatures. For example, in order to model the evolution of aqueous alkaline solutions at high ionic strength, special alkaline ions and species were included into the database, based on recent literature. In particular, virial parameters for following four systems are added: (1) polymerized silica species at high-ionic-strength at ambient temperature (22-25^{o}C) (Felmy et al., 2001); (2) sodium phosphate species in the system Na-PO_4-HPO_4-OH-H_2O, their temperature-dependences are obtained from Weber (2000); (3) the sodium aluminosilicate species in the system Na-$Al(OH)_4$-SiO_3-OH-CO_3-SO_4-HS-Cl (Park and Englezos, 1999); and (4) species involved in Na-H_2SiO_4 and Na-H_3SiO_4 compounds (Hershey and Millero, 1986).

The Pitzer virial parameters are temperature and pressure dependent. The ionic activity coefficients and their partial molal volumes at any given temperature are conventionally obtained by calculating Pitzer' parameters and the Debye-Hückel slopes. Temperature-dependence of the virial parameters can thus be expressed using the derivative terms of enthalpies and heat capacities with respect to temperature. The first order derivative terms of virial parameters with respect to temperature for the selected inorganic compounds at 298.15K were reported (Silvester and Pitzer, 1978). Although in the past decade, a number of studies have focused on the thermodynamic properties of CAS (Pitzer, 1991), no acceptable model currently exists for correlating the available data for solutions over a sufficient large temperature range. Instead, individual and arbitrary equations were often used to describe this dependence, based on interpolations and extrapolations of the experimental data. The interpolation and extrapolation equations for various thermodynamic properties of aqueous solutions for binary and ternary systems and for multiple-component mixtures within the Pitzer formulation

have been reported in many papers (Harvie et al., 1984; Pabalan and Pitzer, 1987; Harvie et al., 1987; Moller, 1988; Greenberg and Moller, 1989; Monnin, 1989 and 1995; Pitzer, 1991; Weber et al., 1999). These authors utilized a variety of activity data, enthalpy data, and heat capacities to construct comprehensive equations over the temperature range of 0 to 250°C. For example, Pabalan and Pitzer (1991) fitted their experimental results with equations using more than 20 adjustable parameters. Moller (1988) and Greenberg and Moller (1989) used an equation with ten adjustable parameters to describe the temperature-dependent parameters (Azaroual et al., 1997). In the present paper, we use the following general algebraic equation:

$$P(T) = P_{T_0} + a_1(T - T_0) + a_2(\frac{1}{T} - \frac{1}{T_0}) + a_3 ln(\frac{T}{T_0}) + a_4(T^2 - T_0^2) \quad (6)$$

where $P(T)$ represents Pitzer parameters $\beta^{(o)}$, $\beta^{(1)}$, $\beta^{(2)}$, and C^{Φ}_{MX} at temperature T (absolute temperature); T_0 is the reference temperature (298.15K used in the database). The polynomial coefficients a_1, a_2, a_3 and a_4 in equation (6) are adjustable fitting coefficients according to experimental data. P_{T_0} is the Pitzer virial parameters at the reference temperature. Equation (6) is valid in a temperature range of 0 - 100 °C. Reasonable estimates of adjustable parameters need to be made over the entire temperature range. These adjustable parameters are stored in the database.

The dependency on pressure is not considered in the present model because: (1) within the normal natural pressure range (100 kPa±50 kPa under laboratory conditions and less than 1,000 kPa under natural groundwater system condition), the dependency of the Pitzer virial parameters on pressure is less significant than that on temperature within the possible temperature range under laboratory and natural conditions (–60 to +100°C) and; (2) fewer experimental data are available for the pressure dependency.

Since most data are obtained from experiments for single or binary electrolytes at ambient temperature, extrapolation of these data to higher temperature and mixed solutions may be unreliable (Lu et al., 1996). In addition, there are little or no thermodynamic data available for aqueous complexes. As stated before, the Pitzer ion-interaction model involves at least five parameters. These parameters were often obtained by the fitting of the experimental data. Accuracy of the simulation at higher concentrations is unknown. The Pitzer formulation is generally applicable in the range 0 <I<6

M, although it may often be used at higher ionic strengths provided that some modifications were made (Weber, 2000; Perez-Villasenor, 2002). In addition, Pitzer virial parameters are available at ambient temperatures for a number of compounds. However, it is also difficult to extend these parameters to higher temperature. Pitzer virial parameters over the range of temperatures is needed to model complex natural systems at variable temperatures. An additional problem affecting the precision of the Pitzer ion-interaction model is the large diversity of the parameters (Krumgalz, 2001). Often, Pitzer virial parameters differ considerably from author to author (Pitzer, 1991; Marshall et al., 1995).

5. Test of the Model

Two cases are presented here to test the Pitzer-type ion-interaction model implemented in BIO-CORE$^{2D©}$. The extensive tests and validations of BIO-CORE $^{2D©}$ dealing with reactive biogeochemical transport problems have been previously performed against analytical solutions (Sun et al, 1999) and numerical solutions from other codes (Zhang, 2001), which are beyond the scope of this paper.

5.1. Hydrochloric Acid in Concentrated Electrolyte Solutions

The measured mean activity coefficients of hydrochloric acid in ternary aqueous solutions of HCl-NaCl-KCl-H_2O and HCl-$BaCl_2$-KCl-H_2O at constant total ionic strengths of 4, 5, 6, and 7 mol/kg and at a temperature of 298.15 K have been previously reported (Jiang, 1996). Here, we use these measured data to test our Pitzer-type ion-interaction model.

To maintain a constant value for the total ionic strength of the system, changes in concentration of KCl are inversely proportional to those of HCl. Figure 1 shows variations of the mean activity coefficient of HCl in a HCl-$BaCl_2$-KCl-H_2O system as a function of concentrations of HCl at 298.15 K. Similarly, Figure 2 presents variations of the mean activity coefficient of HCl in a HCl-NaCl-KCl-H_2O system as a function of concentrations of HCl at 298.15 K. In Figure 2, NaCl replaces $BaCl_2$ in Figure 1. Excellent agreement between the experimental data and our model predictions was obtained at 4 M and 5 M of the total ionic strengths. At higher ionic strength, our model

predictions also are reasonably well compared with the experimental data. Figures 1 and 2 also indicate that our model predictions are better than those from PHRQPITZ (Plummer et al., 1988). Large discrepancies were observed between Debye-Hückel results and the experimental data. It can be seen clearly that the Debye-Hückel model is unable to describe the variation in individual ionic activity, as the total ionic strength remains constant in the system.

5.2. Activity Coefficient of NaCl in Aqueous Solutions at Varying Temperatures

Galleguillos-Castro et al. (1999) conducted a thermodynamic study for the solution system of NaCl-Na_2SO_4-H_2O under four different temperatures. Using the same ion-interaction parameters reported in their paper, we calculated the mean activity coefficients of NaCl at two temperatures. Results are presented in Figure 3 for 25^oC and Figure 4 for 45^oC. The total ionic strength was remained. Therefore, the mean activity coefficient of NaCl will change according to the ionic strength ratio of NaCl and Na_2SO_4. The measured data of mean activity coefficients of NaCl at two temperatures reported in the literature were well reproduced by BIO-CORE $^{2D©}$. Slight differences between model results and experimental data are (in general) within the combined uncertainties of analytical techniques and calculation methodology. Once again, our model results fit experimental data better than those of PHRQPITZ.

6. Application to the Highly Saline Waste Solutions at Hanford

At the U.S. Department of Energy's Hanford site (Richland, Washington), highly alkaline waste solutions (often > 5 M of $NaNO_3$) are stored in 149 single-shell and 28 double-shell underground tanks. Sixty-seven single-shell tanks have been identified as leaking and have released an estimated 1 million gallons of mixed waste solutions into the vadose (unsaturated) zone sediments underneath the tanks. Understanding the chemistry of these saline $NaNO_3$ solutions and how they interact with sediments is important for assessing the contaminant migration and developing remedial actions. For this purpose, a laboratory column experiment was performed using sediment from the Hanford site and a synthetic aqueous solution similar to the Hanford tank fluid. Here, we report this experiment results and the simulations to illustrate and validate our Pitzer-type reactive geochemical transport model.

6.1. Problem setup

The sediment used in this experiment consists of more than 90% of fine quartz sand and clays. The porous medium has a Cation Exchange Capacity (CEC) of 10 meq/100g and contained 7% moisture. An electrolyte fluid of 4 mol/L of $NaNO_3$ and 1 mol/L of NaOH with an ionic strength of 5 M was injected into the bottom of the column. The effluent fluid was collected at the top. A constant injection rate of 0.0432L/d was applied. The injection led to the bottom becomes saturated first, and the wetting front gradually moving upward. Fluid outflow from the top was observed at approximately 0.5 pore volume with the displaced native soil water at the front. The experimental conditions and parameters of fluid flow and chemical transport are listed in Table 1. Details regarding the experimental setup have been described by Wan et al. (2004). Because of the small size and the relatively small flow rate, hydraulic dispersion is expected to play a limited role and thus, the dispersivity is assigned a very small value of 0.002 m. A value of 10^{-9} m^2/s for diffusion was used in the simulation. The bottom of the column was treated as flux boundary for both fluid flow and chemical transport while the top was open for the fluid outflowing.

Effluent pH and concentrations provide information of the processes taking place inside the column when the CAS contacts with the sediment. Especially, the pH breakthrough is a combined effect of a number of geochemical processes. The very high pH in the influent fluid was first declined by quartz dissolution, cation exchange (release H^+ from the sediment), and precipitation of calcite, dolomite, and talc. After a complete washout of the exchangeable cation, the pH recovered. Finally, the previously precipitated calcite, dolomite, and talc were dissolved again and washed out while quartz was kept dissolving.

Major geochemical processes considered in the simulation are given in Figure 5. Aqueous species, minerals, exchanged cations, and some reaction parameters are summarized in Table 2. A total of 9 aqueous component species and 23 aqueous complexes were considered. One primary mineral, quartz, was used and its dissolution was kinetically controlled. The dissolution rate used is: rate = $5\times10^{-8}[OH^-]^{0.5}$ mol/s/dm^2 (Wan et al., 2004), and the reactive surface area was estimated to be 50,000 dm^2 per dm^3 of sand. A total of five secondary minerals (portlandite, sodiumsilicate, talc,

dolomite, and calcite) were considered. Precipitation of these minerals was assumed at local equilibrium. A total of four exchangeable cations: H^+, Na^+, Ca^{+2}, Mg^{+2} were considered.

6.2. Results and Discussion

Figure 6 shows the simulated effluent pH, together with measured values. The Pitzer-type activity model implemented in BIO-CORE$^{2D©}$ captures measured pH values better than the Debye-Hückel model. Figure 7 shows concentration breakthrough for N_a^+, C_a^{+2}, and M_g^{+2}. Figure 8 shows mineral precipitation and dissolution trends inside the column. The high concentration of N_a^+, NO_3^- and OH^- in the injected water causes the monotonic increase in the concentration of these components inside the column and also the effluent after a certain time. The high concentration of N_a^+ replaces the exchangeable C_a^{+2}, M_g^{+2} and H^+ on the solid complex, leading to the increase of C_a^{+2}, M_g^{+2}, and H^+ concentrations in the liquid phase. Peaks of C_a^{+2} and M_g^{+2} concentrations caused by this processes, as well as the decrease of pH, can be clearly seen in Figure 7. These effects observed at the outlet occur just after one pore volume (Figures 6 and 7), because the injected water has very low concentrations of C_a^{+2}, M_g^{+2}, and H^+, and thus dilutes the solution after the exchangeable C_a^{+2}, M_g^{+2} and H^+ on the solid complex are exhausted. The pH is also constrained by mineral dissolution and precipitation. Quartz initially present in the column dissolves more quickly in this high alkalinity condition. The concentration of aqueous silica sharply increases just behind the wetting front. Consequently, talc precipitation occurs where the aqueous silica front mixes with the M_g^{+2} peak. Dolomite and calcite also precipitate in the same manner where M_g^{+2} and C_a^{+2} peaks mix the initial higher concentration of HCO_3^-. Precipitation of these minerals removes OH^- from the solution and thus pH decreases. The complete exhaust of exchangeable C_a^{+2} and M_g^{+2} behind the plume front (caused by lower concentrations of C_a^{+2}, M_g^{+2}, and HCO_3^- in the injection solution) results in the early precipitated talc, with dolomite and calcite dissolving again. Although the concentrations of C_a^{+2} and M_g^{+2} were not measured in this experiment, the simulated trends were observed in similar laboratory experiments conducted at 70 ^{o}C (Wan et al., 2004b).

6.3. Sensitivity analyses

The Major geochemical processes in this application are cation exchange, kinetic dissolution of quartz, and equilibrium precipitation of five minerals. The variations of parameters involved in these processes may span a large range under the conditions tested. To identify main processes affecting the plume development of alkaline solution and the possible range of key parameters, a total of three sensitivity simulations were performed by either systematic removing of relevant processes or varying the values of parameters.

The first sensitivity simulation excluded mineral dissolution/precipitation. Figure 9 shows that simulated pH is at first constant, and then quickly reaches the injected level. The decreasing region of pH observed at around one pore volume becomes very slight (about 15% of the observed pH dropdown magnitude). The peaks of Ca^{+2} and Mg^{+2} concentrations resulting from cation exchange are elevated to varying degrees (not shown). This simulation cannot reproduce the measured pH breakthrough. The mineral dissolution and precipitation is very important because: (1) quartz dissolution provides aqueous silica to precipitate talc with the released Mg^{+2} from the solid surface complex, and sodiumsilicate with the injected Na^{+}, and these precipitations removes OH^{-} causing pH decrease; (2) the released Ca^{+2} and Mg^{+2} from the solid surface complex are also precipitated, to form calcite, dolomite together with the HCO_3^{-} appeared in the sand moisture, and these precipitations also remove OH^{-} causing pH decrease; (3) released Ca^{+2} from the solid surface complex directly precipitated, together with OH^{-} to form portlandite causing pH decrease. If there were not quartz dissolution, there would not be aqueous silica, talc and sodiumsilicate would not precipitate. If there were not precipitation of talc, sodiumsilicate, calcite and dolomite, OH^{-} would not be removed and pH would not decrease in such a magnitude.

The second sensitivity simulation took away cation exchange reactions. The decreasing region of pH (Figure 6) and peaks of Ca^{+2} or Mg^{+2} concentrations (Figure 7) disappears after one pore volume because there were no H^{+} released to decline the pH, and no Ca^{+2} and Mg^{+2} released to precipitate minerals removing OH^{-}.

The third sensitivity simulation used a kinetic rate constant of quartz dissolution decreased by one order of magnitude from the base simulation. The results show that the simulated pH evolution is highly sensitive to the kinetic rate of quartz dissolution. The smaller kinetic rate leads to a higher pH before one pore volume and a smaller pH drop after one pore volume. This is because the smaller dissolution rate causes a lower concentration of aqueous silica and less precipitation of talc and sodiumsilicate. Consequently, a smaller amount of OH^- was removed and a higher pH was obtained (Figure 9). Thus, dissolution of quartz and precipitation of other minerals are essential in this geochemical system. However, the kinetic rate of quartz dissolution greatly depends on the specific surface area and solution chemistry (Rimstidt and Barnes, 1980; Dove, 1994; Rimstidt, 1997). The surface area of quartz is a sediment-type-dependent parameter requiring independent estimation or measurement.

The sensitivity simulations indicate that pH is strongly influenced by cation exchange and mineral dissolution and precipitation. The sensitivity analysis results also suggest that the high alkaline solution leaking into subsurface environment could induce strongly coupled geochemical processes, driving the development of waste plume.

7. Conclusions

We have incorporated a comprehensive Pitzer ion-interaction model into an existing reactive biogeochemical transport code, BIO-CORE$^{2D©}$, to simulate the coupled transport and chemical reactions of aqueous solutions at high-ionic-strength taking place in natural and engineered systems. The model was tested against two reported cases with observation data. The measured data of mean activity coefficients were well reproduced by BIO-CORE $^{2D©}$. Our model results match experimental data better than those of the previous code PHRQPITZ.

The developed model was applied to simulate a laboratory column experiment, injecting a high alkaline (5 M $NaNO_3$) solution into sediment from Hanford site to fake the leaking processes of the high alkaline solutions stored at Hanford site. We found that this Pitzer-type model implemented in BIO-CORE$^{2D©}$ captures measured pH values better than the Debye-Hückel model. The simulation indicates that exchanges of the injected N_a^+ with exchangeable H^+, C_a^{+2} and M_g^{+2} on the solid surface

complex, quartz dissolution, and talc, dolomite and calcite precipitation are strongly coupled. Quartz dissolution provides a source of aqueous silica, the injected Na^+ replaces Ca^{+2}, Mg^{+2}, and H^+ on the solid surface complex and releases them into the solution, and the precipitation of talc, calcite, dolomite, sodiumsilicate and portlandite remove OH^- from the solution, leading to the pH decrease at the time of about 1 pore volume. All these reaction processes contribute to the pH evolution. Sensitivity analyses indicated that the major (~85%) contribution to the pH decrease was from the calcium and magnesium mineral precipitation that removes OH^-, and the directly released H^+ from the solid surface complex replaced by the injected Na^+ is a minor contribution to the pH decease. However, the Ca^{+2} and Mg^{+2} were also sourced from solid surface complex through cation exchanges with Na^+. The remaining problem is that we don't clearly know the contributions from precipitations of each individual mineral to the OH^- removal and the competition between the precipitations, although the precipitation of talc, among other mineral precipitations, is found to remove a larger amount of OH^-. More sensitivity analyses are needed to obtain better understanding.

Appendix A. Debye-Hückel Formula for Activity Coefficient

For non-concentrated solutions (the ionic strength smaller than 1 M), values of the activity coefficient can be commonly calculated according to the extended Debye-Hückel formula, which are expressed as

$$log\,\gamma_i = -\frac{Az_I^2(I)^{\frac{1}{2}}}{1+Ba_i(I)^{\frac{1}{2}}} + bI \qquad \text{(A1)}$$

where I is the ionic strength of the solution; z_i and a_i are the electric charge and the ionic radius of i^{th} aqueous species, respectively; A and B are constants that depend on the temperature and dielectric constant of water, and b is a constant determined from fitting experimental data. The values of A, B, and b at different temperatures are tabulated in Helgeson and Kirkham (1974). The value of the ionic strength is calculated as:

$$I = \frac{1}{2}\sum_{i=1}^{N_T} c_i z_i^2 \tag{A2}$$

The activity of water can be calculated according to Garrels and Christ (1965) as:

$$a_{H_2O} = 1 - 0.018\sum_{i=2}^{N_T} c_i \tag{A3}$$

where i includes all the species in solution except water.

Appendix B. Definition of Coefficients in the Pitzer Virial Equations

Coefficient *Z*, in front of C_{ca}, in Equations (2) is given by:

$$Z = \sum_{k=1}^{N} |z_k| m_k \tag{B1}$$

where z_k and m_k are the electrical charge, and molality of kth species, respectively.

A^{Φ} is one third of the Debye-Hückel limiting slope and is temperature-dependent with a value of 0.392 at 25^{o}C and 1 atm. The temperature-dependence of A^{Φ}, according to Clegg and Whitfield (1991), is given by

$$A^{\Phi} = \begin{cases} 0.13422(0.0368329T - 14.62718\ln T - \dfrac{1530.1474}{T} + 80.40631) & (-60^oC \le T \le 0^oC) \\ 0.13422(4.1725332 - 0.1481291\sqrt{T} + 1.5188505\times10^{-5}T^2 & \\ -1.8016317\times10^{-8}T^3 + 9.3816144\times10^{-10}T^{3.5}) & (-0^oC \le T \le 100^oC) \end{cases} \tag{B2}$$

where T is absolute temperature.

The modified Debye-Hückel term used in Equations (3), (4) and (5) are defined as:

$$F = -A^{\Phi}\left(\frac{\sqrt{I}}{1+1.2\sqrt{I}} + \frac{2}{1.2}ln(1+1.2\sqrt{I})\right) + \sum_{c=1}^{N_c}\sum_{a=1}^{N_a} m_c m_a B'_{ca} \tag{B3}$$

All Pitzer virial coefficients, B^{Φ}_{ca}, B_{MX} (representing B_{Ma} and B_{cX}), $B^{'}_{MX}$ (representing $B^{'}_{Ma}$ and $B^{'}_{cX}$), α_{MX}, and C_{MX} (representing C_{Ma}, C_{cX} and C_{ca}) in Equations (2), (3), (4) and (6) are defined as:

$$B^{\Phi}_{ca} = \beta^{(0)}_{MX} + \beta^{(1)}_{MX} e^{-\alpha_{MX}\sqrt{I}} + \beta^{(2)}_{MX} e^{-\alpha^{'}_{MX}\sqrt{I}} \tag{B4}$$

$$B_{MX} = \beta^{(0)}_{MX} + \beta^{(1)}_{MX} g(\alpha_{MX}\sqrt{I}) + \beta^{(2)}_{MX} g(\alpha^{'}_{MX}\sqrt{I}) \tag{B5}$$

$$B^{'}_{MX} = \beta^{(1)}_{MX} \frac{g'(\alpha_{MX}\sqrt{I})}{I} + \beta^{(2)}_{MX} \frac{g'(\alpha^{'}_{MX}\sqrt{I})}{I} \tag{B6}$$

The function g(x) and g'(x) are given by:

$$g(x) = 2\frac{(1-(1+x)e^{-x})}{x^2} \tag{B7}$$

$$g'(x) = -2\frac{(1-(1+x+\frac{x^2}{2})e^{-x})}{x^2} \tag{B8}$$

where x in Equations (13) and (14) denotes $\alpha_{MX}\sqrt{I}$ or $\alpha^{'}_{MX}\sqrt{I}$. For any salt containing a monovalent ion α_{MX} = 2 and $\alpha^{'}_{MX}$=12; for 2-2 electrolytes α_{MX} = 1.4 and $\alpha^{'}_{MX}$=12; for 3-2 and 4-2 electrolytes α_{MX} = 2.0 and $\alpha^{'}_{MX}$=50 (Silvester and Pitzer, 1978).

The thermodynamic properties of single-salt solutions, C_{MX}, are given by:

$$C_{MX} = \frac{C^{\Phi}_{MX}}{2\sqrt{|z_M z_X|}} \tag{B9}$$

Therefore, defining the activity coefficients and osmotic coefficients for an aqueous solution requires estimates of $\beta^{(0)}_{MX}$, $\beta^{(1)}_{MX}$, $\beta^{(2)}_{MX}$, C^{Φ}_{MX} and λ_{MX}, representing λ_{nc}, λ_{na}, λ_{nM}, λ_{nX}, λ_{Nc} and λ_{Na} in Equations (2) through (5) for the appropriate solution ions.

In all the above formulations, parameters $\beta^{(0)}_{MX}$, $\beta^{(1)}_{MX}$, $\beta^{(2)}_{MX}$, C^{Φ}_{MX} and λ_{nc}, λ_{na}, λ_{nM}, λ_{nX}, λ_{Nc} and λ_{Na} are dimensionless; m_i, m_c, m_a and I are molalities, but also treated as dimensionless variables in the formulations.

Acknowledgement

We thank Daniel Hawkes, Tianfu Xu, and Tetsu K. Tokunaga for internal review of the manuscript and suggestions for improvements. This work was supported by the U.S. Department of Energy, under Contract No. DE-AC03-76SF00098 with Lawrence Berkeley National Laboratory.

References

Azaroual, M., C. Fouillac and J. M. Matray, Solubility of silica polymorphs in electrolyte solutions, 1. Activity coefficient of aqueous silica from 25 ^{o}C to 250 ^{o}C, Pitzer's parameterisation, *Chem. Geol*., 140, 155-165, 1997.

Bethke, C. M., Geochemical Reaction Modeling: Concepts and Applications, Oxford University Press, New York. ISBN 0-19-509475-1, pp 397, 1996.

Blowes, D. W., E. J. Reardon, J. L. Jambor, and J. A. Cherry, The formation and potential importance of cemented layers in inactive sulfide mine tailings. *Geochim. Cosmochim. Acta,* 55, 965-978, 1991.

Boufadel, M. C., M. T. Suidan, and A. D. Venosa, A numerical model for density-and-viscosity-dependent flows in two-dimensional variably saturated porous media, *J. Contam Hydrol*., 37, 1-20, 1999.

Clegg, S. L., and M. Whitfield, Activity coefficients in natural waters, In *Activity Coefficients in Electrolyte Solutions*, edited, K.S. Pitzer, 2nd ed, CRC Press, 1991.

Dougherty, R. C., Density of Salt Solution: Effects of Ions on the Apparent Density of Water, *j. Phys. Chem. B* 2001, 105, 4514-4519, 2001.

Dove, P. M., The dissolution kinetics of quartz in sodium chloride solutions at 25 to 300°C. Am. J. Sci., 294, 665-712, 1994.

Felmy, A. R., GMIN, A computerized chemical equilibrium program using a constrainted minimization of the Gibbs free energy: summary report, *Soil Science Society of America, Special publication,* 42, 377-407, 1995.

Galleguillos-Castro, H. R., F. Hernandez-luis, L. Fernandez-merida, and M. A. Esteso, Thermodynamic study of the NaCl+Na_2SO_4+H_2O system by Emf measurements at four temperatures, *J.Solu. Chem*., 28, 791-807, 1999.

Garrels, R. M., and C. L. Christ, "Solutions, minerals and equilibria", Freeman, Cooper, San Francisco, 450 pp, 1965.

Gephart, R. E., and R. E. Lundgren, *Hanford Tank Cleanup*, Battelle, Columbus, OH., 1998.

Gerson, A. R., and K. Zheng, Bayer process plant scale: transformation of sodalite to cancrinite, *J.Cryst.Growth*, 171, 209-218, 1997.

Greenberg, J. P., and N. Moller, The prediction of mineral solubilities in natural waters: a chemical equilibrium model for the Na-K-Ca-Cl-SO_4-H_2O system to high concentration from 0 to 250 ^oC. *Geochim. Cosmochim.Acta*, 53, 2503-2518, 1989.

Harvie, C. E., and J. H. Weare, The prediction of mineral solubilities in natural waters; the Na-K-Mg-Ca-Cl-SO_4-H_2O system from zero to high concentration at 25 ^oC, *Geochim. Cosmochim.Acta,* 44, 981-997, 1980.

Harvie, C. E., N. Moller, and J. H. Weare, The prediction of mineral solubilities in antural waters: the Na-K-Mg-Ca-H-Cl-SO_4-OH-HCO_3-CO_3-H_2O-system to high ionic strengths at 25 ^oC, *Geochim. Cosmochim.Acta*, 48, 723-751, 1984.

Harvie, C. E., J. P. Greenberg, and J. H. Weare, A chemical equilibrium algorithm for highly nonideal multiphase systems: free energy minimization, *Geochim. Cosmochim Acta*, 51-1045, 1987.

Helgeson, H. C., and D. H. Kirkham, Theoretical prediction of the thermodynamic behaviour of aqueous electrolytes at high pressures and temperatures: II. Debye-Hückel parameters for activity coefficients and relative partial molal properties. Am. J. Sci., 274: 1199-1261, 1974.

Hershey, J. P., and F. J. Millero, The dependence of the acidity constants of silicic acid on NaCl concentration using Pitzer's equations, *Marine Chemistry* 18,101-105, 1986.

Herbert, A.W., C. P. Jackson, and D. A. Lever, Coupled groundwater flow and solute transport with fluid density strongly dependent upon concentration, *Water Resour. Res*., 24, 1781-1795, 1998.

Jiang, C., Activity coefficients of hydrochloric acid in concentrated electrolyte solutions. 2. HCl+$BaCl_2$+KCl+H_2O, HCl+LiCl+KCl+H_2O, and HCl+NaCl+KCl+H_2O at 298.15K, *J.Chem.Eng.Data*, 41, 117-120, 1996.

Krumgalz, B. S., Application of the Pitzer ion-interaction model to natural hypersaline brines, *J.Molecular Liquids*, 91,3-19, 2001.

Lichtner, P. C., *FLOTRAN user manual*, LA-UR-01-2349, Los Alamos national Laboratory, Los Alamos, New Mexico, 2001.

Lichtner, P. C., and A. Felmy, Estimation of Hanford SX tank waste compositions from

historically derived inventories, *Computer&Geosciences*, 2002.

Lu, X., L. Zhang, Y. Wang, J. Shi, and G. Maurer, Prediction of activity coefficients of electrolytes in aqueous solutions at high temperatures. *Ind. Eng.Chem.Res*. 35,1777-1784, 1996.

Marshall, S. L., P. M. May, and G. T. Hefter, Least-squares analysis of osmotic coefficient data at 25 ^{o}C according to Pitzer'equation.1. 1:1 electrolytes., *J.Chem.Eng.Data*, 40, 1041-1052, 1995.

Moller, N., The prediction of mineral solubilities in natural waters : a chemical equilibrium model for the Na-Ca-Cl-SO_4-H_2O system to high temperature and concentration, *Geochim. Cosmochim.Acta*, 52, 821-837, 1988.

Monnin, C., An ion-interaction model for the volumetric properties of natural waters: density of the solution and partial molal volumes of electrolytes to high concentrations at 25 ^{o}C, *Geochim. Cosmochim. Acta,* 53, 1177-1188, 1989.

Monnin, C., 1994, Density calculation and concentration scale conversions for natural waters, *Computers and Geosciences*, 20, 1435-1445, 1994.

Oldenburg, C. M., and K. Pruess, Dispersive transport dynamics in a strongly coupled groundwater-brine flow system, *Water Resour. Res*., 31, 289-302, 1995.

Pabalan, R. T., and K. S. Pitzer, Thermodynamics of concentrated electrolyte mixtures and the prediction of mineral solubilities to high temperatures for mixtures in the system Na-K-Mg-Cl-SO_4-OH-H_2O. *Geochim. Cosmochim.Acta*, 51, 2429-2443, 1989.

Park H., and P. Englezos, Thermodynamic modeling of sodium aluminosilicate formation in aqueous alkaline solutions, *Ind. Eng. Chem. Res*., 38, 4959-4965, 1999.

Perez-Villasenor F., G. A., Iglesias-Silva, and K. R. Hall, Osmotic and activity coefficients using a modified Pitzer equation for strong electrolytes 1:1 and 1:2 at 298.15K, *Ind. Eng.Chem.Res.*, 41, 1031-103, 2002.

Pitzer, K. S., Thermodynamics of electrolytes, 1, Theoretical basis and general equations, *J.Phys.Chem*., 77, 268-277, 1973.

Pitzer, K. S., Ion interaction approach: theory and data correlation. In *Activity Coefficients in Electrolytes Solutions*, edited by K.S. Pitzer, 2nd, CRC Press, 75-155, 1991.

Pitzer, K. S., and J. J. Kim, Thermodynamics of electrolytes. IV. Activity and osmotic coefficients for mixed electrolytes. *J.Am.Chem. Soc*., 96, 5701-5707,1974.

Pitzer, K. S., and G.Mayorga, Thermodynamics of electrolytes.II.activity and osmotic coefficients for strong electrolytes with one or both ions univalent, *J. Phy.Chem.,* 77,2300-2307, 1973.

Plummer, L. N., D. L. Parkhurst, G. W. Fleming, and S. A. Dunkle, *A computer program incorporating Pitzer's equations for calculation of geochemical reactions in brines,* United States Geological Survey Water Resources Investigation Report 88-4153, 1-310,1988.

Rimstidt, J. D., and H. L. Barnes, The kinetics of silica-water interaction. Geochim. Cosmochim. Acta, 1980, 44, 1683-1699, 1980.

Rimstidt, J.D., Quartz solubility at low temperatures. Geochim. Cosmochim. Acta, 61,2553-2558, 1997.

Risacher, F., and A. Clement, A computer program for simulation of evaporation of natural waters to high concentration, *Computers & Geosciences*, 27,191-201, 2001.

Samper, J., R., Juncosa, J. Delgado, and L. Montenegro, $CORE^{2D}$: A code for non-isothermal water flow and reactive solute transport. Users manual version 2. ENRESA Technical Publication 06/2000. 131 pp, 2000.

Simunek, J., and L. Suarez, Two-dimensional transport model for variably saturated porous media with major ion chemistry, *Water Resour. Res*., 30(4), 1115-1131, 1994.

Silvester, L. F., and K. S., Pitzer, Thermodynamics of electrolytes. 10. Enthalpy and the effect of temperature on the activity coefficients, *J. Solu. Chem*., 7, 327-337, 1978.

Steefel C. I., S. Carroll, P. Zhao, and S. Roberts, Cesium migration in Hanford sediment: a multisite cation exchange model based on laboratory transport experiment. J. Contam. Hydrol. 67, 219-246, 2003.

Sun Y., J. N. Petersen, T. P. Clement, and R. S. Skeen, Development of analytical solutions for multi-species transport with serial and parallel reactions, *Water Resources Research*, Vol. 35, No. 1, pp. 185-190, 1999.

Van Gaans, P.F.M., and R. D. Schuiling, The waste sulfuric acid lake of the TiO_2-plant at Armyansk, Crimea, Ukraine, II. modeling the chemical evolution with PHRQPITZ, *Appl. Geochem*., 12, 187-201, 1997.

Voss, C.I., and W.R., Souza, Variable density flow and solute transport simulation of regional aquifers containing a narrow freshwater-saltwater transition zone, *Water Resour. Res*., 23, 1851-1866, 1987.

Wan, J., J. T., Larsen, T. K., Tokunaga, and Z. Zheng, pH neutralization and zonation in alkaline-saline tank waste plumes. Environ. Sci. Technol. 38, (in press) 2004.

Wan, J., T. K. Tokunaga, J.T. Larsen, and R. J. Serne, Geochemical evolution of highly alkaline and saline tank waste plumes during seepage through vadose zone sediments. Geochim. Cosmochim. Acta. 68, 491-502, 2004.

Weber, C.F., E. C., Beahm, and J. S., Watson, Modeling thermodynamics and phase equilibria for aqueous solutions of trisodium phosphate, *J.Solu. Chem*, 28, 1207-1237, 1999.

Weber, C.F., 2000, calculation of Pitzer parameters at high-ionic-strengths*, Ind.Eng.Chem.Res*, 39, 4422-4426.

Wolery T. J., and S. A. Daveler, EQ6, A Computer program for Reaction Path Modeling of Aqueous Geochemical System: Theoretical Manual, User's Guide, and Related Documentation (version 7.0) *Lawrence Livermore National Laboratory*, 1992.

Xu T., J. Samper, C. Ayora, M. Manzano, and E. Custodio, Modeling of Non-Isothermal Multi-Component Reactive Transport in Field Scale Porous Media Flow System *J. Hydrol*, 214(1-4), 144-164, 1999.

Yeh, G.T., and V. S. Tripathi, "A model for simulating transport of reactive multispecies components: model development and demonstration", *Water Resour. Res.* 27(12), 3075-3094,1991.

Zhang, G., Nonisothermal Hydrobiogeochemical Models in Porous Media Ph.D. dissertation, University of La Coruña, Spain, pp368, 2001.

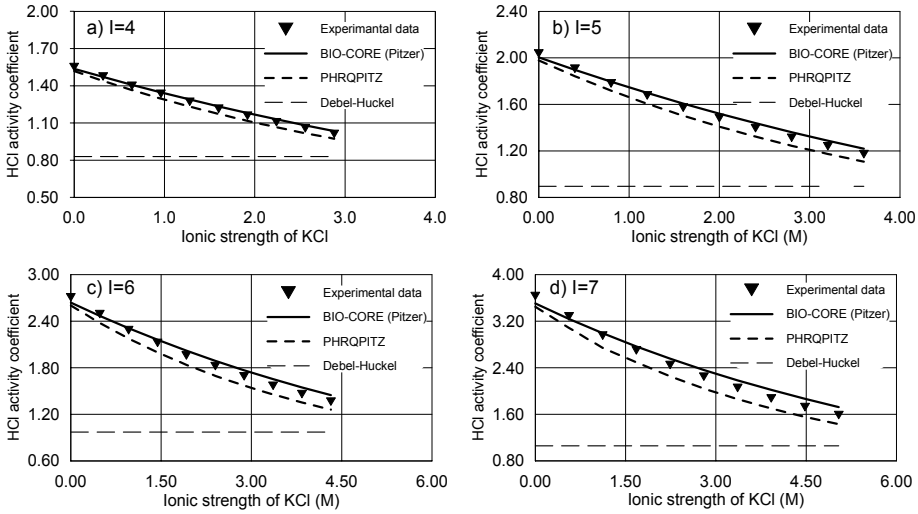

Figure 1. Comparison of measured and calculated ionic activity coefficients of HCl in an HCl-$BaCl_2$-KCl-H2O system as a function of the concentration of KCl for total ionic strength of 4, 5, 6 and 7 m, respectively

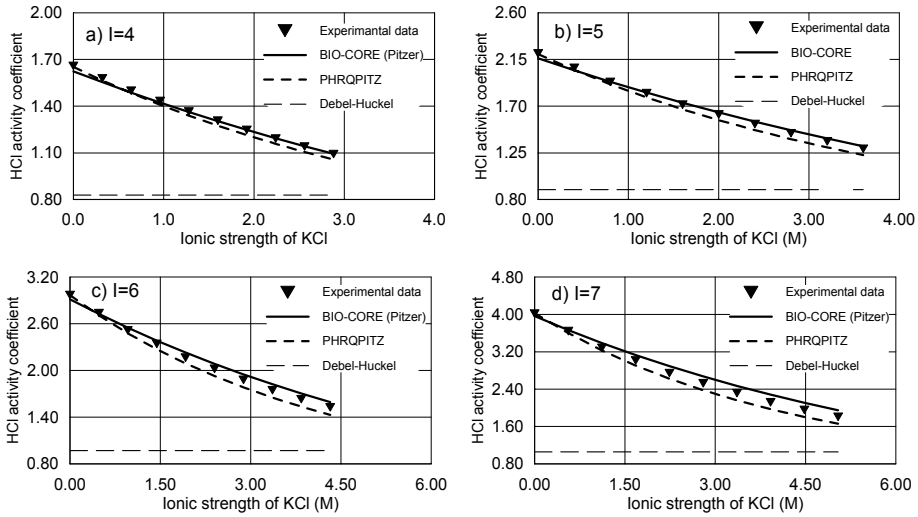

Figure 2. Comparison of measured and calculated ionic activity coefficients of HCl in an HCl-NaCl-KCl-H2O system as a function of the concentration of KCl for total ionic strength of the solution at 4, 5, 6 and 7 M, respectively

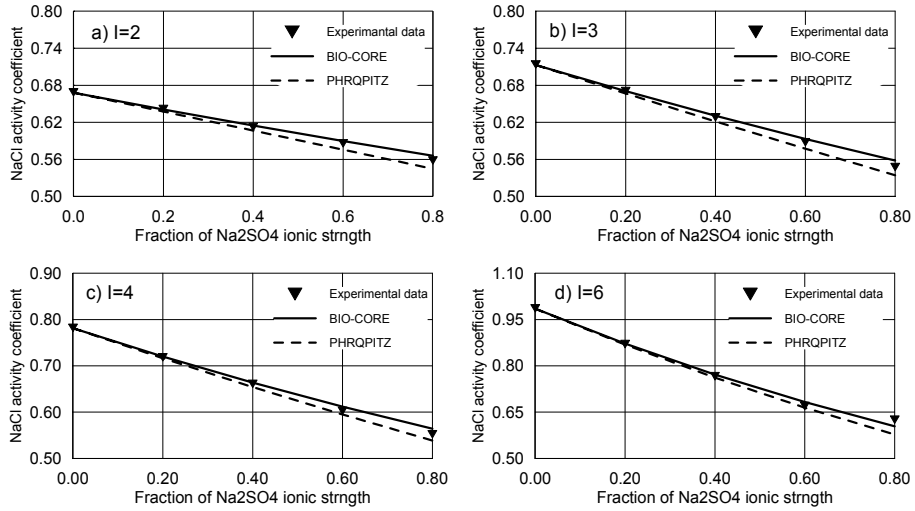

Figure 3. Comparison of measured and calculated mean ionic activity coefficients of NaCl in an NaCl-Na_2SO_4-H_2O system as a function of fraction of Na_2SO_4 ionic strength at 25°C and total solution ionic strength of 2, 3, 4, and 6 M, respectively

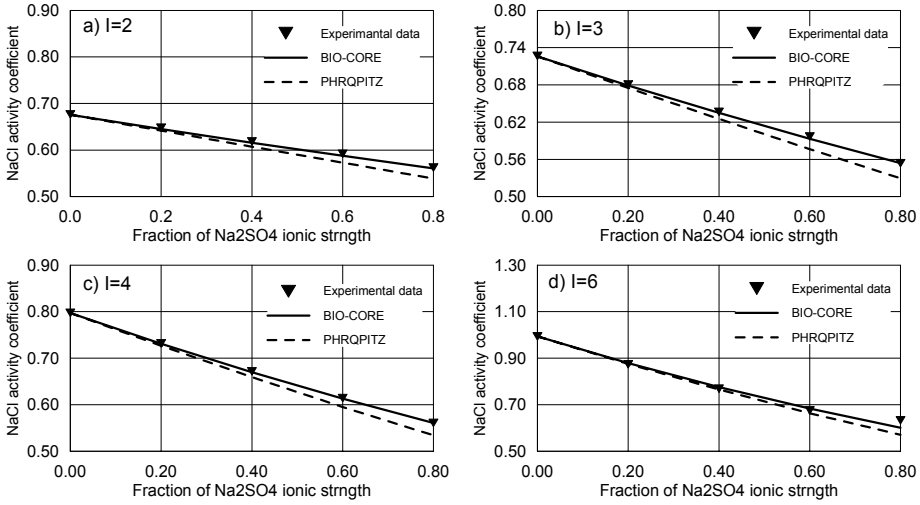

Figure 4. Comparison of measured and calculated mean ionic activity coefficients of NaCl in NaCl-Na_2SO_4-H_2O system as function of fraction of Na_2SO_4 ionic strength at 45°C and total solution ionic strength of 2, 3, 4, and 6 M, respectively

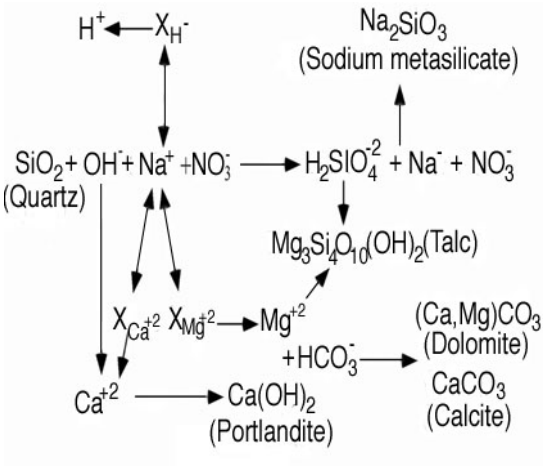

Figure 5. Mayor geochemical processes taking place in the column system, $X_{C_a^{+2}}$, $X_{M_g^{+2}}$ and X_{H^+} represent the exchangeable cations

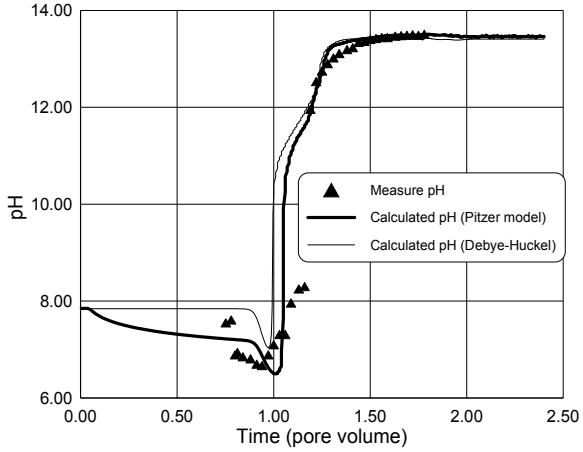

Figure 6. Simulated effluent pH compared to measured data

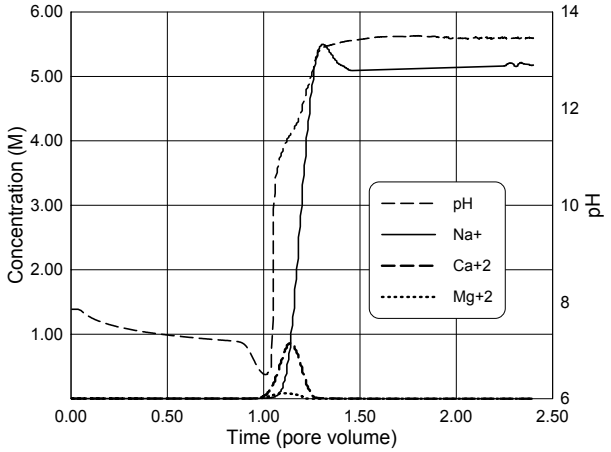

Figure 7. Breakthrough curves calculated for effluent concentrations of N_a^+, C_a^{+2}, M_g^{+2} and pH

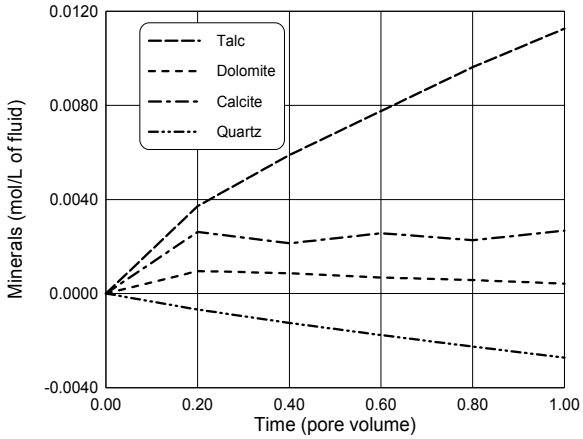

Figure 8. Simulated accumulative minerals precipitation (positive) and dissolution (negative) at different times (spatially maximum values)

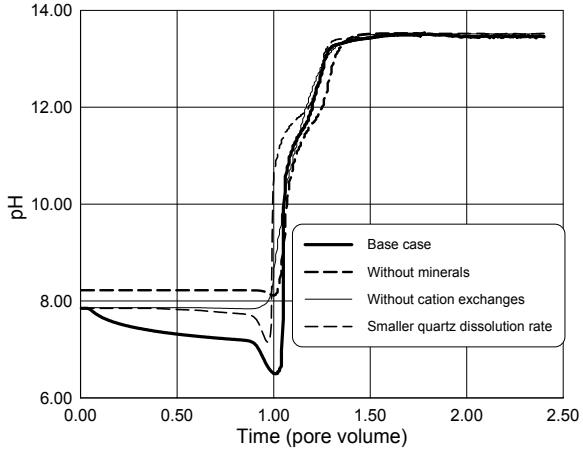

Figure 9. Sensitivity analyses of calculated pH with respect to mineral dissolution/precipitation, cation exchanges, and smaller kinetic rate of quartz dissolution (one order of magnitude)

Table 1. Experimental conditions and hydrological parameters used in the model

Column size	0.25 m (length)×0.038m(diameter), spatial discretization with Δx = 0.0025cm
Filled material	quartz (mass fraction F_m>90%, average diameter of particles, φ=0.2 mm, surface area, A_s=50,000 dm2/dm3 porous medium); density, ρ=1.72kg/L; porosity, ϕ=0.4; initial saturation, S_0=25%; residual saturation, S_r=7%.
Flow parameters	flow rate=0.0432L/d; permeability=0.64 m/d; van Genuchten m=0.731; van Genuchten α =9.0 m^{-1}.
Transport parameters	diffusion coefficient, $D_0=10^{-9} m^2/s$; dispersivity, α_L =0.002m.

Table 2. Summary of the chemical system in the model

Components	**H_2O**	**H^+**	**Na^+**	**Ca^{+2}**	**Mg^{+2}**	**NO_3^-**	**HCO_3^-**	**SO_4^{-2}**	**$SiO_{2(aq)}$**	
Concentrations in the column pore water (M/L)	1.0	6.01×10^{-09}	1.18×10^{-03}	4.48×10^{-04}	2.12×10^{-04}	1.00×10^{-10}	1.38×10^{-03}	5.60×10^{-04}	1.074×10^{-04}	pH=8.221
Concentrations of the injected fluid (M/L)	1.0	4.0×10^{-14}	5.0	1.0×10^{-10}	1.0×10^{-10}	4.0	1.0×10^{-10}	1.0×10^{-10}	1.0×10^{-10}	pH=13.398
Aqueous complexes	**Stoichiometric coefficients**									**Log (K)**
OH^-	1.00	-1.00	0.00	0.00	0.00	0.00	0.00	0.00	0.00	1.3997E+01
CO_3^{-2}	0.00	-1.00	0.00	0.00	0.00	0.00	1.00	0.00	0.00	1.0339E+01
HSO_4^-	0.00	1.00	0.00	0.00	0.00	0.00	0.00	1.00	0.00	-1.9791E+00
$H_3SiO_4^-$	2.00	-1.00	0.00	0.00	0.00	0.00	0.00	0.00	1.00	9.8120E+00
$H_2SiO_4^{-2}$	2.00	-2.00	0.00	0.00	0.00	0.00	0.00	0.00	1.00	2.2912E+01
$NaOH_{(aq)}$	1.00	-1.00	1.00	0.00	0.00	0.00	0.00	0.00	0.00	1.4180E+01
$NaHCO_{3(aq)}$	0.00	0.00	1.00	0.00	0.00	0.00	1.00	0.00	0.00	-1.5410E-01
$NaCO_3^-$	0.00	-1.00	1.00	0.00	0.00	0.00	1.00	0.00	0.00	9.8249E+00
$NaSO_4^{-2}$	0.00	0.00	1.00	0.00	0.00	0.00	0.00	1.00	0.00	-8.2000E-01
$NaHSiO_{3(aq)}$	1.00	-1.00	1.00	0.00	0.00	0.00	0.00	0.00	1.00	8.3040E+00
$NaH_3SiO_{4(aq)}$	2.00	-1.00	1.00	0.00	0.00	0.00	0.00	0.00	1.00	8.6616E+00
$CaOH^+$	1.00	-1.00	0.00	1.00	0.00	0.00	0.00	0.00	0.00	1.2850E+01
$CaNO_3^+$	0.00	0.00	0.00	1.00	0.00	1.00	0.00	0.00	0.00	-7.0000E-01
$CaHCO_3^+$	0.00	0.00	0.00	1.00	0.00	0.00	1.00	0.00	0.00	-1.0467E+00
$CaCO_{3(aq)}$	0.00	-1.00	0.00	1.00	0.00	0.00	1.00	0.00	0.00	7.1880E+00
$CaSO_{4(aq)}$	0.00	0.00	0.00	1.00	0.00	0.00	0.00	1.00	0.00	-2.1111E+00
$Ca(H_3SiO_4)_{2(aq)}$	4.00	-2.00	0.00	1.00	0.00	0.00	0.00	0.00	2.00	1.5053E+01
$MgOH^+$	1.00	-1.00	0.00	0.00	1.00	0.00	0.00	0.00	0.00	1.1787E+01
$MgHCO_3^+$	0.00	0.00	0.00	0.00	1.00	0.00	1.00	0.00	0.00	-1.0357E+00
$MgCO_{3(aq)}$	0.00	-1.00	0.00	0.00	1.00	0.00	1.00	0.00	0.00	7.3604E+00
$MgSO_{4(aq)}$	0.00	0.00	0.00	0.00	1.00	0.00	0.00	1.00	0.00	-2.4117E+00
$Mg(H_3SiO_4)_{2(aq)}$	4.00	-2.00	0.00	0.00	1.00	0.00	0.00	0.00	2.00	1.3723E+01
$CO_{2(aq)}$	-1.00	1.00	0.00	0.00	0.00	0.00	1.00	0.00	0.00	-6.3375E+00
Minerals	**Stoichiometric coefficients**									**Log (K)**
Quartz	0.00	0.00	0.00	0.00	0.00	0.00	0.00	0.00	1.00	rate = $5\times10^{-8}[OH^-]^{0.5}$ mol/s/dm^2
Portlandite ($Ca(OH)_2$)	2.00	-2.00	0.00	1.00	0.00	0.00	0.00	0.00	0.00	2.2555E+01
Sodiumsilicate (Na2sio3)	1.00	-2.00	2.00	0.00	0.00	0.00	0.00	0.00	1.00	2.2241E+01
Talc	4.00	-6.00	0.00	0.00	3.00	0.00	0.00	0.00	4.00	2.1138E+01
Dolomite	0.00	-2.00	0.00	1.00	1.00	0.00	2.00	0.00	0.00	2.5135E+00
Calcite	0.00	-1.00	0.00	1.00	0.00	0.00	1.00	0.00	0.00	1.9330E+00
Exchangeable cations	**CEC (meq/100g solid)**							**Equilibrium constant**		
H^+ (master)	0.0027							1		
Na^+	0.2023							0.99		
Ca^+	7.5500							0.20		
Mg^+	2.2450							0.40		

Table 3. Virial coefficients of the major ionic pairs for the Pitzer model used in the simulations (25°C)Table 3. Virial coefficients of the major ionic pairs for the Pitzer model used in the simulations (25°C)

		OH^-	SO_4^{-2}	HSO_4^-	CO_3^{-2}	HCO_3^-	NO_3^-	$H_3SiO_4^-$	$H_2SiO_4^{-2}$
H^+	β_0		0.2980E-01►	0.2065E+00►			0.1119E+00►		
	β_1		0.0000E+00►	0.5556E+00►			0.3206E+00►		
	β_2		0.0000E+00►	0.0000E+00►			0.0000E+00►		
	C		0.4380E-01►	0.0000E+00►			0.1000E-02►		
N_a^+	β_0	0.8640E-01▲	0.1958E-01▲	0.4540E-01▲	0.3990E-01▲	0.2770E-01▲	0.6800E-02►	0.4300E-01▼	0.3200E+00◄
	β_1	0.2530E+00▲	0.1113E+01▲	0.3980E+00▲	0.1389E+01▲	0.4110E-01▲	0.1783E+00►	0.2400E+00▼	0.1300E+00◄
	β_2	0.0000E+00▲	0.0000E+00▲	0.0000E+00▲	0.0000E+00▲	0.0000E+00▲	0.0000E+00►	0.0000E+00▼	0.0000E+00◄
	C	0.4400E-02▲	0.4970E-02▲	0.0000E+00▲	0.4400E-02▲	0.0000E+00▲	-.7200E-03►	0.0000E+00▼	0.0000E+00◄
C_a^{+2}	β_0	-.1747E+00▲	0.2000E+00▲	0.2145E+00▲		0.4000E+00▲	0.2108E+00▲		
	β_1	-.2303E+00▲	0.3197E+01▲	0.2530E+01▲		0.2977E+01▲	0.1409E+01▲		
	β_2	-.5720E+01▲	-.5424E+02▲	0.0000E+00▲		0.0000E+00▲	0.0000E+00▲		
	C	0.0000E+00▲	0.0000E+00▲	0.0000E+00		0.0000E+00▲	-.2014E-01▲		
M_g^{+2}	β_0		0.2210E+00▲	0.4746E+00▲		0.3290E+00▲	0.3670E+00□		
	β_1		0.3343E+01▲	0.1729E+01▲		0.6072E+00▲	0.1580E+01□		
	β_2		-.3723E+02▲	0.0000E+00▲		0.0000E+00▲	0.0000E+00□		
	C		0.2500E-01▲	0.0000E+00▲		0.0000E+00▲	0.2060E-01□		
Reference: ▲: Plummer et al., (1988); ►:Pitzer (1991); ▼: Hershey and Millero (1986); ◄: Bickmore (2001); □: Risacher and Clement (2001)									

Table 4. λ parameters of mayor aqueous molecules and ions interactions for the Pitzer model used in the simulations (25°C)

	$CO_{2(aq)}$	$SiO_{2(aq)}$
H^+		
N_a^+	0.1000E+00♦	0.9250E-01▲
C_a^{+2}	0.1830E+00♦	0.6590E-01▲
M_g^{+2}	0.1830E+00♦	0.6000E-01▼
OH^-		0.1816E+00▲
SO_4^{-2}	0.9700E-01♦	0.2000E-01▼
HSO_4^-	-.3000E-02♦	
HCO_3^-		0.1500E-01
NO_3^-		0.3610E-01▼
Reference: ▲: Azaroual et al. (1997); ▼: Risacher and Clement (2001); ♦: Plummer et al. (1988)		